Measurement of the b Quark Fragmentation Function in Z^0 Decays

D.N. Dong
Massachusetts Institute of Technology

We present preliminary results of a new measurement of the b quark fragmentation function in Z^0 decays using a novel kinematic B hadron energy reconstruction technique. The measurement is performed using 150,000 hadronic Z^0 events recorded in the SLD experiment at SLAC between 1996 and 1997. The small and stable SLC beam spot and the CCD-based vertex detector are used to reconstruct topological B-decay vertices with high efficiency and purity, and to provide precise measurements of the kinematic quantities used in this technique. We measure the B energy with good efficiency and resolution over the full kinematic range. We compare the scaled B hadron energy distribution with several functional forms of the B hadron energy distribution and predictions of several models of b quark fragmentation. Several functions including JETSET + Peterson are excluded by the data. The average scaled energy of the weakly decaying B hadron is measured to be $x_B = 0.719 \pm 0.005$ (stat) $\pm$ 0.007 (syst) $\pm$ 0.001 (model) (preliminary).

I. INTRODUCTION

The fragmentation process which transforms colored partons into colorless hadrons is typically characterized by the fragmentation function. The b quark fragmentation is of special importance in the study of quark fragmentation because the large b quark mass provides a natural mass scale in QCD calculations and allows the application of perturbative QCD and heavy quark expansion, and can help to extract non-perturbative effects in fragmentation, which is the least understood part of the fragmentation process.

According to the factorization theorem, the heavy quark fragmentation function can be described as a convolution of perturbative and non-perturbative effects. For the b quark, the perturbative calculation is in principle understood [1–5]. Nonperturbative effects have been parametrized in both model-dependent [6–10,1] and model-independent approaches [2–5]. The fact that several models are yet to be experimentally tested is an indication of a lack of precise and conclusive experimental results, if not theoretical understanding.

It is indeed experimentally challenging to measure the b quark fragmentation function to a level of precision sufficient to distinguish among the various models. Since the b quark fragmentation function is the probability distribution of the fraction of the momentum of the b quark carried by the B hadron, the most sensitive experimental determination of the shape of the b fragmentation function is expected to come from a precise direct measurement of the B hadron energy (or momentum) distribution. The difficulty in precisely measuring the B hadron energy distribution stems mostly from the fact that most of the B decays can only be partially reconstructed, causing a significant fraction of the B energy to be missing from the B decay vertex. Recent direct measurements at LEP [11,12] and SLD [13] have used overall energy-momentum constraints and calorimetric information to extract this missing energy in a sample of semi-leptonic B decays. These measurements suffer from low statistics as well as poor B energy resolution at low energy, and hence have a relatively weak discriminating power between different shapes of the fragmentation function. Indirect measurements [14] such as the measurements of the lepton spectrum and charged multiplicity have been used to constrain the average B energy. However, these measurements are not very sensitive to the shape of the energy distribution.

Here we report preliminary results of SLD's new measurement of the B hadron energy distribution. We developed a novel kinematic technique which uses only charged tracks associated with the B vertex and the B flight direction to reconstruct individual B hadron energy with good resolution over the full kinematic range while achieving an efficiency much higher than previous measurements.

II. B HADRON SELECTION

A general description of the SLD detector can be found elsewhere [16,17] The excellent tracking and vertexing capabilities at SLD [18] are exploited in the reconstruction of B decays in $Z^0 \to b\,\bar{b}$ events.

A set of cuts is applied to select hadronic Z^0 events well-contained within the detector acceptance. The efficiency for selecting a well-contained $Z^0 \to q\bar{q}(g)$ event is estimated to be above 96% independent of quark flavor. The selected sample comprise 111,569 events, with an estimated $0.10 \pm 0.05\%$ background contribution dominated by $Z^0 \to \tau^+\tau^-$ events.

The B sample is selected using a topological vertexing technique based on the detection and measurement of charged tracks, which is described in full detail in Ref. [19]. The topological vertexing algorithm [19] is applied separately to the set of "quality" tracks in each hemisphere (defined with respect to the event thrust axis). When a candidate vertex is found, tracks not associated with this "seed" vertex are attached to the vertex if they are more likely to have originated from this vertex than from the IP. This track-attachment procedure is tuned to minimize false track-vertex associations to the vertex. Attaching a false track to the vertex affects the vertex-kinematics more than failing to associate a genuine track originated from the vertex, and hence can cause significant degradation in the reconstructed B energy resolution. On average, this procedure attaches 0.8 tracks to each seed vertex; about 92% of the reconstructed tracks which originated from the B-decay are associated with the reconstructed vertex, and 98% of the vertex-associated tracks are true B decays tracks.

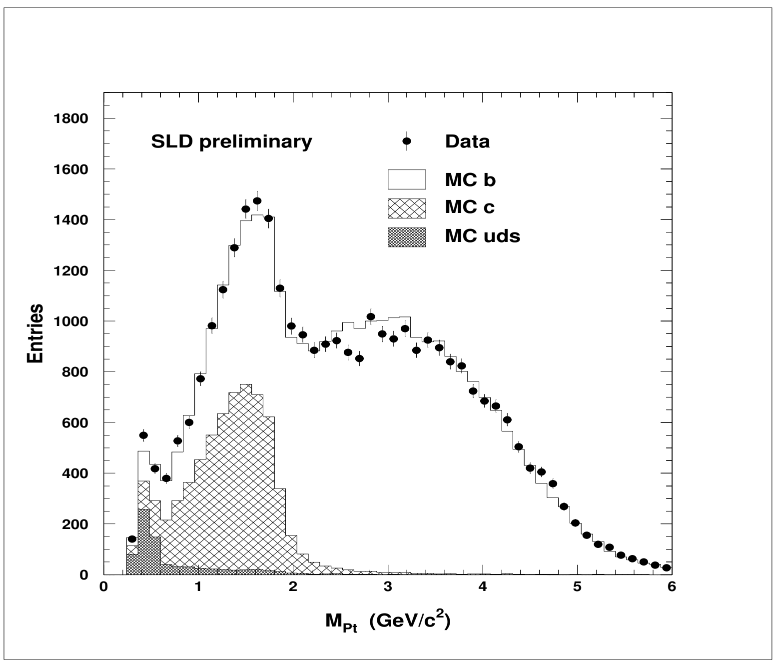

FIG. 1. Distribution of the reconstructed P_t-corrected vertex mass in the 1996-97 data (points). Also shown is the prediction of the Monte Carlo simulation, for which the flavor composition is indicated.

The mass of the reconstructed vertex, M_{ch}, is calculated by assigning each track the charged-pion mass. Because of the tiny SLC IP error and the excellent vertex resolution, the B flight direction pointing along the line joining the IP and the secondary vertex is well-measured. Therefore the transverse momentum P_t of tracks associated with the vertex relative to the B flight direction is also well-measured. The mass of the missing particles can then be partially compensated by using P_t to form the "P_t corrected mass", $M_{P_t} = \sqrt{M_{ch}^2 + P_t^2} + |P_t|$. To minimize effects of large fluctuations of P_t at short decay length, the minimum transverse momentum (which is varied within the 1σ limits constraining the axis at the measured interaction point (IP) and reconstructed seed vertex) is calculated in order to determine M_{P_t}. Figure 1 shows the distribution of the P_t-corrected mass (points) for the 32,492 accepted hemispheres in the data sample, and the corresponding simulated distribution. To obtain a high purity B sample, B hadron candidates are selected by requiring $M_{P_t} > 2.0$ GeV$/c^2$. A total of 19,604 hemispheres are selected, with an estimated efficiency for selecting a true B-hemisphere of 40.1%, and a sample purity of 98.2%. The contributions from light-flavor events in the sample are 0.15% for primary u,d and s events and 1.6% for c events.

III. B ENERGY RECONSTRUCTION

Since the sum of the charged track energy at the B vertex, E_{ch}, is known, we are only concerned with finding the energy of particles missing from the B vertex.

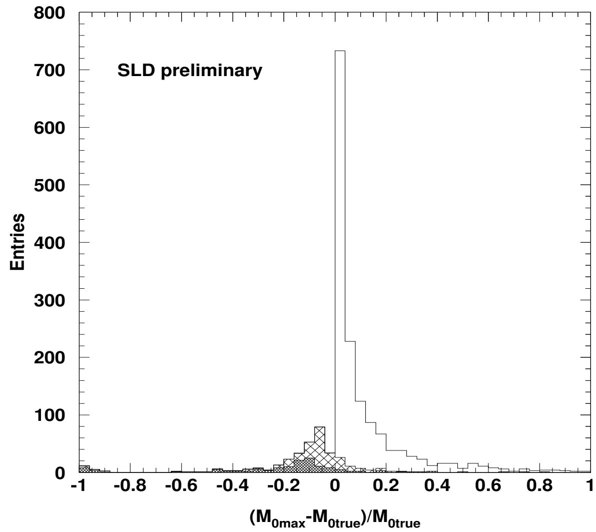

FIG. 2. The relative deviation of the maximum missing mass from the true missing mass for Monte Carlo simulated B hadron decays, which is divided into three categories: B^0 and $B^{\pm}$ (open), B^0_s (cross-hatched), and Λ_b (dark hatched).

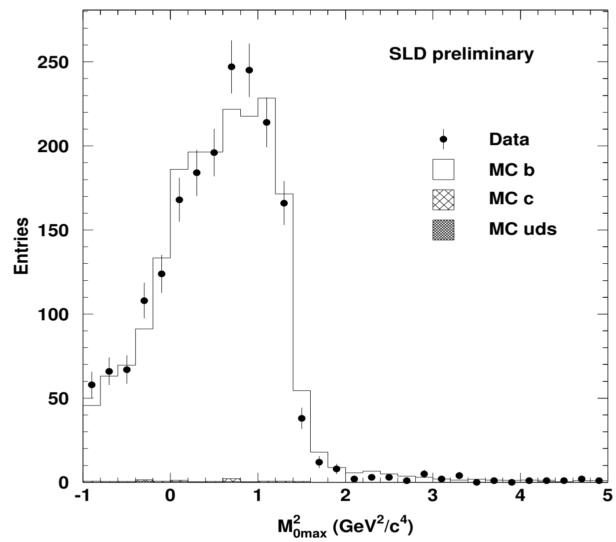

FIG. 3. Distribution of the reconstructed M^2_{0max} for the selected vertices in the 1996-97 data (points). Also shown is the prediction of the Monte Carlo simulation.

Given reconstructed B vertex, an upper bound on the mass of the missing particles from the vertex is found to be $M^2_{0max} = M^2_B - 2M_B\sqrt{M^2_{ch} + P^2_t} + M^2_{ch}$, where we assume the true mass of the B hadron decayed at the vertex, M_B, equals the B^0 meson mass. Since the true missing mass M_0^{true} is often rather close to M_{0max} (Figure 2), M_{0max} is subsequently used as an estimate of M_0^{true} (M_0^{true} is set to 0 if the reconstructed M_{0max} is negative) to solve for the longitudinal momentum of the missing particles from kinematics:

$$P_{0l} = \frac{M^2_B - (M^2_{ch} + P^2_t) - (M^2_0 + P^2_t)}{2(M^2_{ch} + P^2_t)} P_{chl},$$

and hence the missing B energy from the vertex, E_0. The B hadron energy is then $E_B = E_{ch} + E_0$. Since $0 \leq M_0^{true} \leq M_{0max}$, the B energy is well-constrained when M_{0max} is small. In addition, most uds and c backgrounds are concentrated at large M_{0max}. We choose an *ad hoc* upper cut on the M^2_{0max} to achieve a nearly x_B-independent B selection efficiency. Figure 3 shows the distribution of M^2_{0max} after these cuts, where the data and Monte Carlo simulation are in good agreement. A total of 1920 vertices in the 1996-97 data satisfy all selection cuts. Figure 4 shows the distribution of the reconstructed scaled weakly decaying B hadron energy for data and Monte Carlo. The overall B selection efficiency is 3.9% and the estimated purity is about 99.5%. The efficiency as a function of x_B^{true} is shown in Figure 5. We examine the normalized difference between the true and reconstructed B hadron energies for Monte Carlo events. The distribution is fitted by a double Gaussian, resulting in a core width (the width of the narrower Gaussian) of 10.4% and a tail width (the width of the wider Gaussian) of 23.6% with a core fraction of 83%. Figure 6 shows the core and tail widths as a function of x_B^{true}. The core width depends only weakly on the true x_B, another feature that makes this method unique.

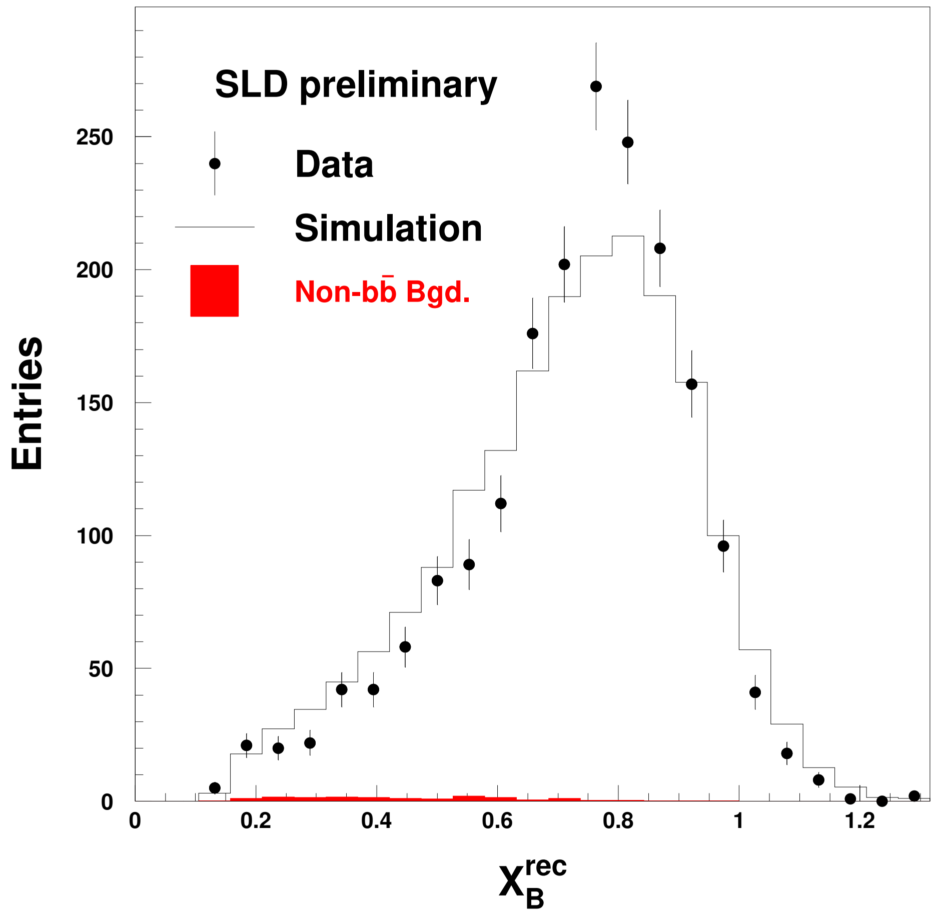

FIG. 4. Distribution of the reconstructed scaled B hadron energy for data(points) and simulation (histogram). The solid histogram shows the non-$b\bar{b}$ background.

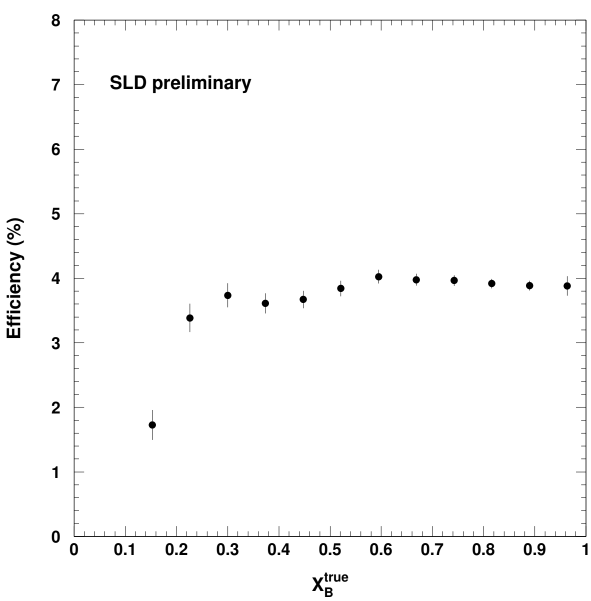

FIG. 5. Distribution of the efficiency as a function of the true B energy.

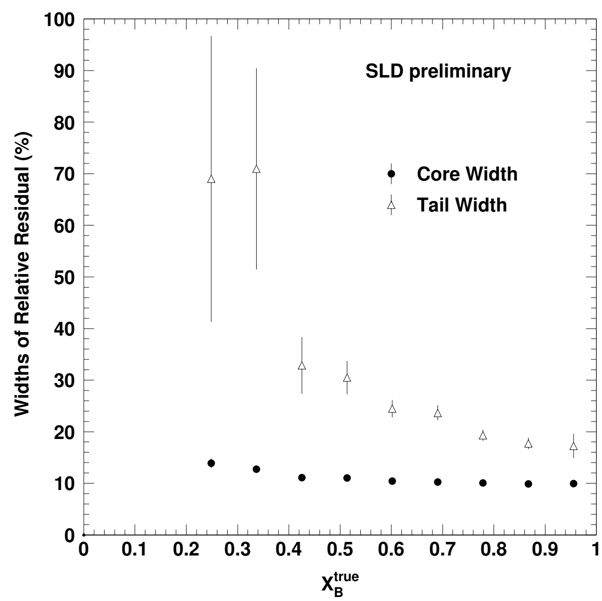

FIG. 6. The fitted core and tail widths of the B energy resolution as a function of the true scaled B hadron energy.

IV. TESTS OF FUNCTIONAL FORMS AND MODELS

After background subtraction, the distribution of the reconstructed scaled B hadron energy is compared with a set of *ad hoc* functional forms of the x_B distribution in order to estimate the variation in the shape of the x_B distribution. For each functional form, the default SLD Monte Carlo is re-weighted and then compared with the data bin-by-bin and a χ^2 is computed. The minimum χ^2 is found by varying the input parameter(s). The Peterson function [8], two *ad hoc* generalizations of the Peterson function [12] (ALEPH 1 and 2) and a 7th-order polynomial [1] are consistent with the data. We exclude the functional forms described in BCFY [4], Collins and Spiller [10], Kartvelishvili [6], Lund [9] and a power function of the form $f(x) = x^{\alpha}(1-x)^{\beta}$. The result is shown in Figure 6 and in Table I and II.

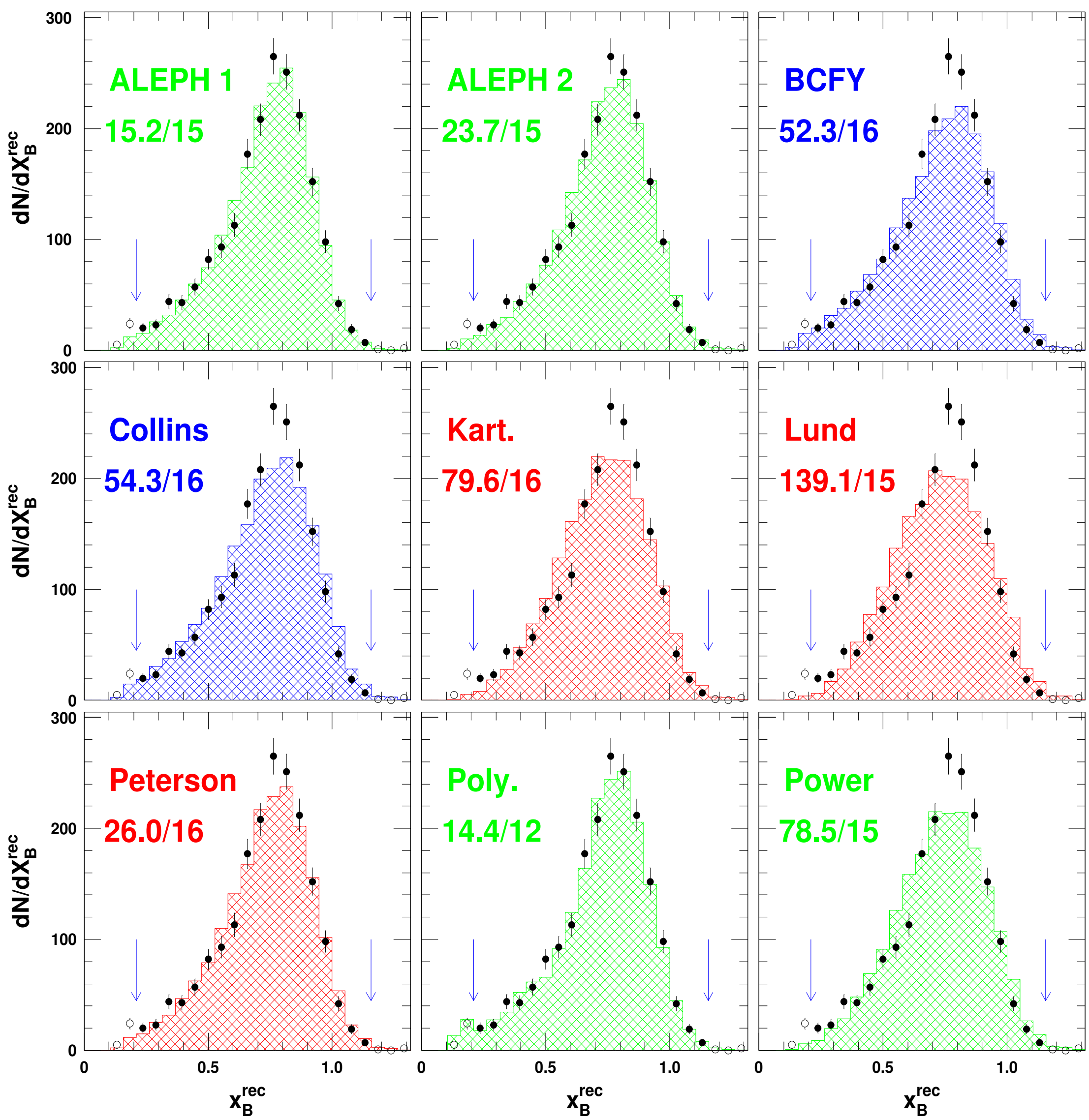

FIG. 7. Each figure shows the background-subtracted distribution of reconstructed B hadron energy for the data (points) and for the simulation (histograms) based on the respective optimised input fragmentation function. The χ^2 fit uses data in the bins between the two arrows.

---

[1]The behavior of this polynomial is rather unphysical at low x_B and will not be considered hereafter

TABLE I. Fragmentation functions used in comparison with the data. For the BCFY function $f_1(r) = 3(3-4r)$, $f_2(r) = 12-23r+26r^2$, $f_3(r) = (1-r)(9-11r+12r^2)$, and $f_4(r) = 3(1-r)^2(1-r+r^2)$. A polynomial function and a power function are also included (see text for discussion).

Function	$D(x)$	Reference
ALEPH	$\frac{1+b(1-x)}{x}(1-\frac{c}{x}-\frac{d}{1-x})^{-2}$	[12]
BCFY	$\frac{x(1-x)^2}{[1-(1-r)x]^6}[3+\sum_{i=1}^{4}(-x)^i f_i(r)]$	[4]
Collins and Spiller	$(\frac{1-x}{x}+\frac{(2-x)\epsilon_b}{1-x})(1+x^2)(1-\frac{1}{x}-\frac{\epsilon_b}{1-x})^{-2}$	[10]
Kartvelishvili *et al.*	$x^{\alpha_b}(1-x)$	[6]
Lund	$\frac{1}{x}(1-x)^a exp(-bm_\perp^2/x)$	[9]
Peterson *et al.*	$\frac{1}{x}(1-\frac{1}{x}-\frac{\epsilon_b}{1-x})^{-2}$	[8]
Polynomial	$x(1-x)(1+\sum_{i=1}^{5} p_i x^i)$	(see text)
Power	$x^\alpha(1-x)^\beta$	(see text)

TABLE II. Results of the χ^2 fit of fragmentation functions to the reconstructed B hadron energy distribution after background subtraction. Minimum χ^2, number of degrees of freedom and coresponding parameter values are listed. Errors are statistical only.

Function	χ^2/dof	Parameters	$\langle x_B \rangle$
ALEPH 1	15.2/15	$c = 0.860^{+0.019}_{-0.018}$	0.718±0.005
		$d = 0.019 \pm 0.002$	
ALEPH 2	23.7/15	$c = 0.938^{+0.039}_{-0.034}$	0.720±0.005
		$d = 0.036 \pm 0.002$	
BCFY	52.3/16	$r = 0.2316^{+0.0092}_{-0.0088}$	0.713±0.005
Collins and Spiller	54.3/16	$\epsilon_b = 0.044^{+0.005}_{-0.004}$	0.714±0.005
Kartvelishvili *et al.*	79.6/16	$\alpha_b = 4.15 \pm 0.11$	0.720±0.004
Lund	139.1/15	$a = 2.116^{+0.118}_{-0.114}$	0.720±0.005
		$bm_\perp^2 = 0.408^{+0.073}_{-0.070}$	
Peterson *et al.*	26.0/16	$\epsilon_b = 0.0338^{+0.0020}_{-0.0022}$	0.719±0.005
Polynomial	14.4/12	$p_1 = -12.4 \pm 0.4$	(see text)
		$p_2 = 58.7 \pm 1.9$	
		$p_3 = -130.5 \pm 4.2$	
		$p_4 = 136.8 \pm 4.3$	
		$p_5 = -53.7 \pm 1.8$	
Power	78.5/15	$\alpha = 3.91^{+0.25}_{-0.24}$	0.722±0.005
		$\beta = 0.894^{+0.102}_{-0.097}$	

We then test several heavy quark fragmentation models. Since the fragmentation functions are usually functions of an experimentally inaccessible variable (e.g. $z = (E+p_\parallel)_H/(E+p_\parallel)_Q$), it is necessary to use a Monte Carlo generator such as JETSET [20] to generate events according to a given input heavy quark fragmentation function. The resulting B energy distribution is then used to re-weigh the Monte Carlo distribution before comparing with the data. The minimum χ^2 is found by varying the input parameter(s). Within the context of the JETSET Monte Carlo, Bowler [7] and the Lund [9] models are consistent with the data, while Peterson [8] model is found to be inconsistent with the data.

V. SYSTEMATIC ERRORS

We have considered both detector and physics modelling systematics. The dominant systematic error is related to charged track transverse momentum resolution smearing, which has been evaluated conservatively and can be reduced with a detailed study. All physics systematics are rather small. Other relevant systematic effects such as by varying the event selection cuts and the assumed B hadron mass are also found to be small. In each case, conclusions about the shape of the B energy distribution hold, and the systematics in the average B hadron energy is added in quadrature to obtain the total systematics.

VI. CONCLUSION

Taking advantage of SLC's small beam-spot and SLD's high vertex resolution, we have developed a new kinematic technique to measure, for the first time, the B hadron energy distribution in Z^0 decays with good resolution over the full kinematic range. Using 1996-97 data, we exclude several functional forms of the B energy distribution and the JETSET + Peterson fragmentation model. The mean of the scaled weakly decaying B hadron energy distribution is obtained by taking the average of the means of the three functional forms which are found to be consistent with the data. The r.m.s. of the three means is regarded as a minimum error on model-dependence. We find

$$< x_B >= 0.719 \pm 0.005(stat) \pm 0.007(syst) \pm 0.001(model)$$

where the small model-dependence error indicates that $< x_B >$ is relatively insensitive to the allowed forms of the shape of the fragmentation function. The precision in the measured average B hadron energy represents a substantial improvement over previous direct measurements. All results are preliminary.

---

[1] B. Mele and P. Nason, Phys. Lett. **B245** (1990) 635.
B. Mele and P. Nason, Nucl. Phys. **B361** (1991) 626.
G. Colangelo and P. Nason, Phys. Lett. **B285** (1992) 167.
[2] R.L.Jaffe, L.Randall, Nucl. Phys. **B412** (1994) 79.
[3] L. Randall, N. Rius, Nucl. Phys. **B441** (1995) 167.
[4] E. Braaten, K. Cheung, T.C. Yuan, Phys. Rev. **D48** (1993) R5049.
E. Braaten, K. Cheung, S. Fleming, T.C. Yuan, Phys. Rev. **D51** (1995) 4819.
[5] Yu. L. Dokshitzer, V.A. Khoze, S.I. Troyan, *Phys. Rev.* D**D53** (1996) 89.
[6] V. G. Kartvelishvili, A. K. Likhoded and V. A. Petrov, Phys. Lett. **78B** (1978) 615.
[7] M.G. Bowler, Z. Phys. **C11** (1981) 169.
[8] C. Peterson, D. Schlatter, I. Schmitt and P.M. Zerwas, Phys. Rev. **D27** (1983) 105.
[9] B. Andersson, G. Gustafson, G. Ingelman, T. Sjöstrand, Phys. Rep. **97** (1983) 32.
[10] P.D.B. Collins and T.P. Spiller, J. Phys. G **11** (1985) 1289.
[11] DELPHI Collab., P. Abreu *et al.*, Z. Phys. **C57** (1993) 181.
[12] ALEPH Collab., D. Buskulic *et al.*, Phys. Lett. **B357** (1995) 699.
[13] SLD Collab., K. Abe *et al.*, Phys. Rev. **D56** (1997) 5310.
[14] ALEPH Collab., D. Buskulic *et al.*, Z. Phys. **C62** (1994) 179.
DELPHI Collab., P. Abreu *et al.*, *Z. Phys.* C**C66** (1995) 323.
L3 Collab., O. Adeva *et al.*, Phys Lett. **B261** (1991) 177.
OPAL Collab., P.D. Acton *et al.*, Z. Phys. **C60** (1993) 199.
[15] SLD Collab., K. Abe *et al.*, SLAC-PUB-7826 (1998).
[16] SLD Design Report, SLAC-Report (1984) 273.
[17] SLD Collab., K. Abe *et al.*, Phys. Rev. **D53** (1996) 1023.
[18] SLD Collab., K. Abe *et al.*, Nucl. Inst. and Meth. **A400**, (1997) 287.
[19] D. J. Jackson, Nucl. Inst. and Meth. **A388**, (1997) 247.
[20] T. Sjöstrand, Comput. Phys. Commun. **82** (1994) 74.